N84-28216

DRL NO. 191/DRD NO.SE5
Line Item No.7

DOE/JPL-956369-84/01
Distribution Category UC-63

MICROCRYSTALLINE SILICON GROWTH FOR HETEROJUNCTION SOLAR CELLS

FINAL REPORT
February 1984

For Period Covering
November 1982 Thru January 1984

By:

D.C. Leung and P.A. Iles
APPLIED SOLAR ENERGY CORPORATION
15251 E. Don Julian
City Of Industry, California 91746

and

P.H. Fang
BOSTON COLLEGE
Chestnut Hill, Mass. 02167

JPL Contract No. 956369

"The JPL Low-Cost Silicon Solar Array Project is sponsored by the U.S. Government of Energy and forms part of the Solar Photovoltaic Conversion Program to initiate a major effort toward the development of low-cost solar arrays. This work was performed for the Jet Propulsion Laboratory, California Institute of Technology by agreement between NASA and DOE."

DRL NO. 191/DRD NO.SE5
Line Item No.7

DOE/JPL-956369-84/01
Distribution Category UC-63

MICROCRYSTALLINE SILICON GROWTH FOR HETEROJUNCTION SOLAR CELLS

FINAL REPORT
February 1984

For Period Covering
November 1982 Thru January 1984

By:

D.C. Leung and P.A. Iles
APPLIED SOLAR ENERGY CORPORATION
15251 E. Don Julian
City Of Industry, California 91746

and

P.H. Fang
BOSTON COLLEGE
Chestnut Hill, Mass. 02167

JPL Contract No. 956369

"The JPL Low-Cost Silicon Solar Array Project is sponsored by the U.S. Government of Energy and forms part of the Solar Photovoltaic Conversion Program to initiate a major effort toward the development of low-cost solar arrays. This work was performed for the Jet Propulsion Laboratory, California Institute of Technology by agreement between NASA and DOE."

ABSTRACT

Microcrystalline Si (m-Si) films with a 1.7eV energy bandgap and crystal size of several hundred Å were e-beam evaporated on single crystalline Si (c-Si) to form a heterojunction with the substrate, or a window layer to a single crystalline p-n junction (heteroface structure). The goal was to enhance Voc by such uses of the larger bandgap m-Si, with the intriguing prospect of forming heterostructures with exact lattice match on each layer.

It was found that the heterojunction structure was affected by interface and shunting problems and the best Voc achieved was only 482mV, well below that of single crystal Si homojunctions. The heteroface structure showed promise for some of the samples with p m-Si/p-n structure (the complementary structure did not show any improvement). Although several runs with different deposition conditions were run, the results were inconsistent. Any Voc enhancement obtained was too small to compensate for the current loss due to the extra absorption and poor carrier transport properties of the m-Si film. A study of the m-Si/c-Si interface using a p-p or n-n heterojunction showed that m-Si did not always serve as a minority carrier barrier as expected. The Voc in many samples was of opposite polarity from that predicted which indicated some degree of carrier collection. This raised problems concerning the nature of the m-Si/c-Si interface. In order for this approach to succeed, these interface problems need to be solved along with improvement of the m-Si layer quality.

TABLE OF CONTENTS

LIST OF FIGURES

LIST OF TABLES

I. INTRODUCTION

The objective of this program is to explore the uses of microcrystal silicon (m-Si) film on single crystalline silicon (c-Si) for solar cell applications, either as a m-Si/c-Si heterojunction or using the m-Si film as a window layer to c-Si p-n junction to enhance solar cell performance. This utilization is possible because m-Si has an optical bandgap of ~1.7eV and under the right circumstances potentially could enhance Voc, e.g. by reducing surface recombination at the interface, with consequent reduced "saturaion current".

The effort on m-Si was directed in two areas:

a) To see if a heterojunction structure could be built which has identical lattice constants on each side of the junction.

b) To see if, in a heteroface structure, the equality of lattice constants can be used to reduce surface recombination at the P^+ surface in a P^+/N cell (analogous to the use of AlGaAs/GaAs).

This program was a joint venture of ASEC and Boston College. The role of Boston College was to deposit and hydrogenate m-Si films on samples and to analyze the films. The role of ASEC was to prepare samples and to fabricate and test cells after m-Si films were deposited on the samples.

In the contract period, a total of 35 runs of film depositions was made at Boston College. The initial co-evaporation procedure using silicon and boron in separated boats was later replaced by a single evaporation of silicon heavily doped with boron, to reduce the chance of carbon contamination from the graphite boron boat. The sample structures included p mSi/n-c-Si and p mSi/p-n-c-Si, with some of the substrates having n^+ back layers included to insure ohmic

back contacts. Also included was a p m-Si/p c-Si structure for testing purposes. Figure 1 shows the three structures. Some parallel tests with m-Si deposited only on part of the p-n junction wafers (with the other part used as control) were also conducted. In the later part of the contract, preliminary tests were also made on structures complementary to those shown in Figure 1, i.e. n-type m-Si films on p substrates, or n-p junctions.

1) HETEROJUNCTION

(COMPLEMENTARY STRUCTURE: n-TYPE m-Si FILM ON p SUBSTRATE)

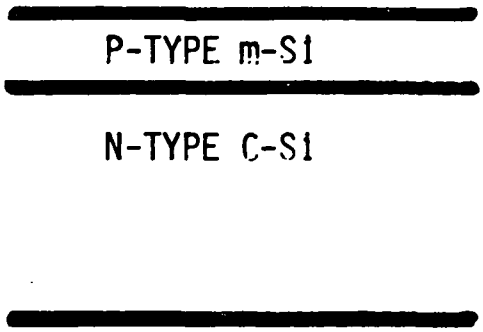

2) HETEROFACE

(COMPLEMENTARY STRUCTURE: n-TYPE m-Si FILM ON n/p JUNCTION SUBSTRATE)

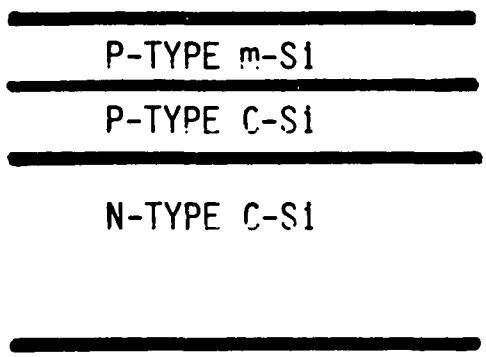

3) p m-Si/p C-Si TESTING STRUCTURE

(COMPLEMENTARY STRUCTURE: n-TYPE m-Si ON n SUBSTRATE)

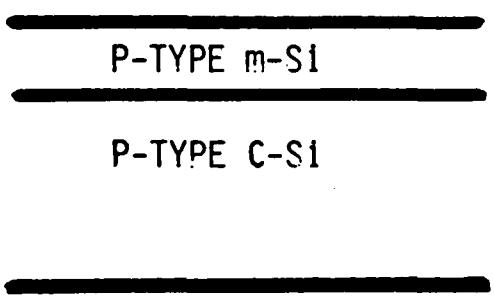

FIGURE 1

VARIOUS STRUCTURES TO BE STUDIED

II. BACKGROUND OF m-Si

During the last few years, there has been a rapid growth of interest on m-Si. This growth is reflected in the Tenth International Conference on Amorphous and LIquid Semiconductors (Aug. 1983, Tokyo) where microcrystals formed a separate topic of the conference. Boston College has been studying polycrystalline silicon since the early seventies. Various methods of deposition have been studied, including electron beam vaporization in vacuum. Presently, work has been concentrated on the electron beam evaporation method. In most of the experiments, steel coated with either silicon oxide or titanium, was used as substrate[1]. The resulting film several microns thick shows, at a sufficiently high substrate temperature, an x-ray diffraction pattern of polycrystal silicon. An x-ray determination indicates that those crystals which have grain sizes of several hundred angstroms have better photovoltaic performance. Another interesting observation[2], is that solar cells made of this material are improved by a hydrogenation treatment, a similar result to that observed for amorphous silicon (a-Si). Based on those results, a paper was published, describing results obtained with these submicron polycrystal silicon solar cells[3].

In the current usage, the term microcrystal is adapted following Nagarta et.al.[4] instead of an accurate, but cumbersome term submicrocrystal as suggested originally.

In the following, some properties of m-Si pertinent to the present program will be reviewed and discussed.

1. Methods Of Preparing m-Si. A discussion of different preparation methods is important because the different properties obtained depend on the preparation methods. There are three methods presently studied:

i. Glow discharge of silane, similar to the process used to prepare a-Si, but at a higher rf power.[4-6]

ii. Chemical transport between a solid silicon charge and the substrate, all in a hydrogen plasma.[7,8]

iii. Electron beam evaporation of solid silicon in vacuum at a substrate temperature above 500°C.[3,9]

The size of these microcrystals varied but generally was in the order of hundreds of Å. This size can be varied by changing the deposition parameters available in different preparation methods.

2. Optical Absorption Spectrum. The wavelength dependence of the absorption coefficient is shown in Figure 2. The main part of this figure is a reproduction from reference 8, superimposed on which are the data from glow discharge and electron beam evaporation. The data from glow discharge are available only in a limited photon energy region[5] and are reproduced as a dashed area with an upper edge for lower rf power and a lower edge for higher rf power. The data from electron beam evaporation are closer to those of glow discharge deposition than those of chemical transport.

In the $(\alpha)^{1/2}$ vs $h\nu$ plot, the chemical transport case gives an optical band gap of 1.1 eV, closer to that of single crystal silicon. On the other hand, the optical band gap values from both glow discharge and e-beam evaporation are very similar, both around 1.7eV. An interpretation of this 1.7 eV gap as a manifestation of the second indirect transition of silicon has been presented elsewhere.[11]

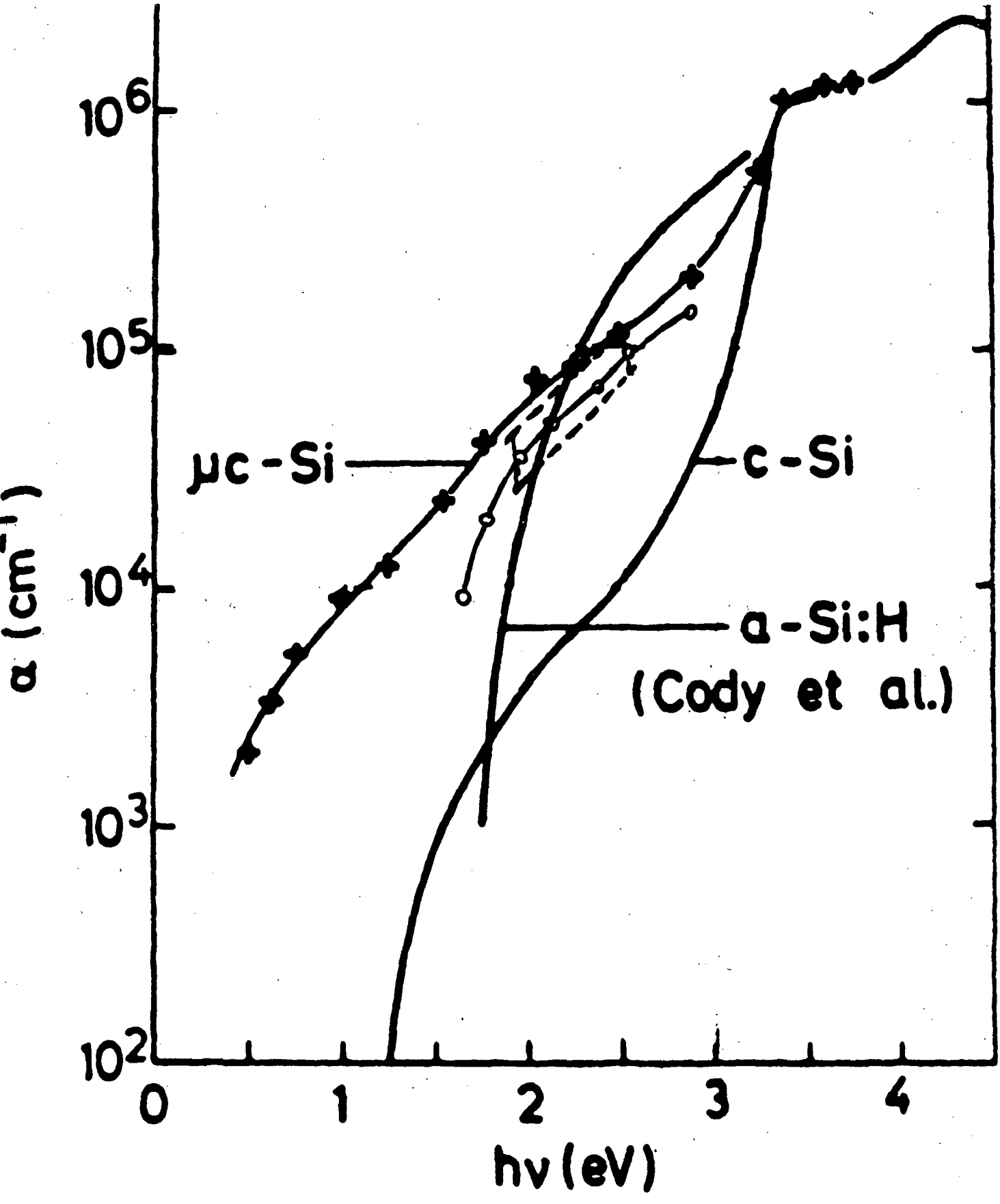

Fig. 2 Optical absorption of microcrystal Si grown by chemical transport (μc-si). Vacuum evaporation (0) and high rf power glow discharge (——). For comparison, amorphous Si:H and crystalline Si also are shown.

There are two points to be observed in the absorption spectrum away from 1.7eV: the mixing effect of m-Si with a-Si and the relation between m-Si with single crystal silicon (c-Si). As shown in Figure 2, there is a transition energy below which the absorption coefficient of m-Si is higher than that of a-Si and above this transition energy the opposite is observed. The value of this transition energy, about 2 eV, is an important region of photon abundance in the solar spectrum and in this respect, m-Si is more favored than a-Si for photovoltaic applications. Also, in comparison with c-Si, in spite of the existence of a prominently higher band gap of 1.7 eV in m-Si, absorption increases much more rapidly than that of single crystals and presumably also than that of large grain polycrystals. Therefore, an m-Si solar cell can be made thinner than c-Si but still produce the same number of electron hole pairs.[3]

3. Doping Effectiveness. Similar to a-Si, m-Si can be doped by the same impurities as those used in the doping of c-Si, but there is a quantitative difference: the effectiveness of a dopant in the host material is described by the ratio of ionized dopant to the total dopant concentration. Denoting by C the impurity concentration to produce a desired electrical conductivity, it was reported that $C_a/C_m \sim C_m/C_c \sim 10^3$ as a first order approximation (where subscript a, m and c stand for a-Si, m-Si and c-Si respectively). Therefore m-Si has much higher conductivity than a-Si for the same level of dopant added. Consequently when devices are made with an electrode contact to a m-Si layer, an ohmic contact can be realized more easily.

4. Transition Region For Growth Of m-Si. In most investigations of m-Si, a foreign substrate such as glass, quartz[10,13] or a metal surface[9,11] is used. The initial growth according to these observations indicates an amorphous state and a transition region, as much as 500Å before a full growth of m-Si. In the present work, single crystal silicon is the substrate, and there are three possibilities: i) an epitaxial growth of single crystal, ii) an amorphous initial state followed by m-Si, and iii) an instantaneous growth of m-Si. The actual condition is important, because in the present application, the thickness of m-Si is planned to be only from 1000 to 3000Å. If a transition region of 500Å is involved, this interfacial state would have a strong influence on the solar cell performance. One experimental approach to verify this problem is an in-situ Raman spectroscopic observation during the growth.[14] Such a complicated evaluation is beyond our scope of investigation at present.

III. VACUUM DEPOSITION SYSTEM AND PREPARATION PROCEDURE

The process to prepare m-Si in the present program is by an electron beam evaporation of solid silicon in vacuum. A schematic figure of the deposition system was shown in Figure 3. The legends are:

(0) Substrates

(1) Steel substrate holder.

(2) Heater made of ceramic plate with molybdenum resistance wire.

(3) Electromagnetic deflector for electron beam.

(4) Tungsten filament for electron emission.

(5) Titanium crucible.

(6) Intrinsic silicon crucible.

(7) p-doped silicon crucible.

(8) Boron source boat (graphite) (later replaced).

(9) Antimony source boat (tantalum).

(10) Shutter

(11) Thermocouple for substrate temperature measurement.

(12) Electrical lead for 2.

(13) Electrical lead for 4 and electron acceleration voltage.

(14) Water cooler for electron beam assembly.

(15) Heat shield cage with port to insert or remove substrates.

(16) Steel belljar.

(17) Plasma generating rod.

This system had been used for a number of years to make silicon thin film solar cells on steel and glass substrates. In the present program, the substrate (0) was single crystal silicon. The crystal had been cleaned by several procedures, and we found that a convenient as well as an effective method was by a plasma cleaning. The complete procedure was detailed below.

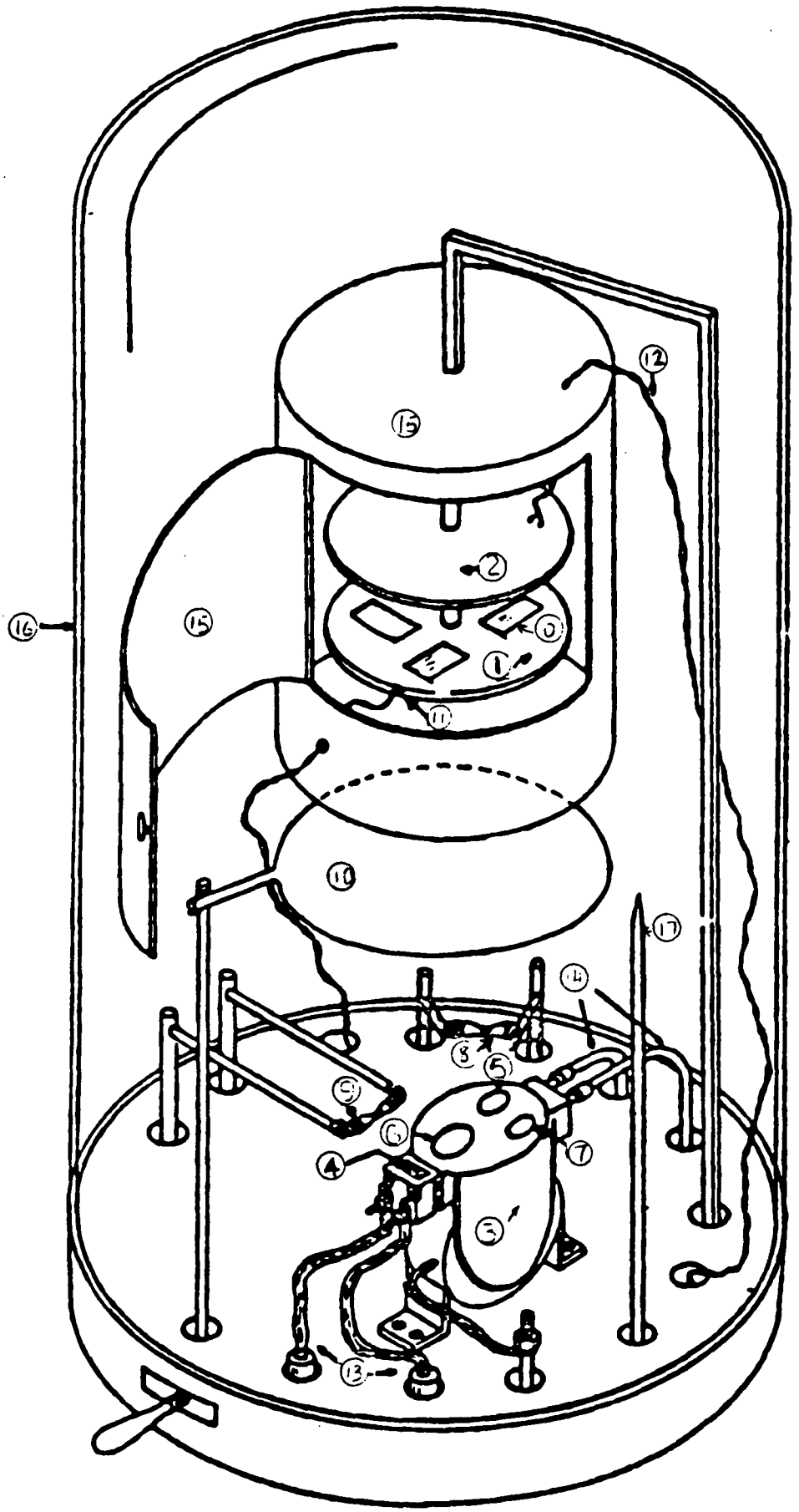

FIGURE 3
EVAPORATION ASSEMBLY

Silicon, supplied by ASEC was placed on a steel substrate holder (1). This substrate holder had five recess frames 1x2 inch in size, and each frame had an open window area of 1.5 x 4.6cm^2 for m-Si deposition. Occasionally one frame out of the five was used for glass slides from which optical studies were made.

After the specimen was placed on (1), part of the heat shield cage (15) was closed and the bell jar (16) was closed. After a pump down to 1x10^{-5} torr by mechanical and oil diffusion pumps, electrical power was supplied to the heater (2). The temperature was measured by a thermocouple attached to (1) near one substrate (0). There was an uncertainty on the exact value of the substrate temperature because of the radiation heat loss from the substrate surface facing downward, the heat reflection from the substrate surface facing upward to the heater (2), and a peripheral contact between the substrate 0 and the frame of the substrate holder (1). However, when this temperature was used as a reference temperature, the measurement could be made with a good repeatability and precision, with an actual value of about 5 to 25^{o}C lower than that from the thermocouple reading.

There was some degassing during the temperature rise. After the temperature reaches an equilibrium value and the vacuum reaches 10^{-5} torr again, hydrogen was leaked into the system to about 100 microns pressure and a plasma was started by a dc voltage of 3 kV with a current of about 10 ma. This plasma cleaning procedure was mostly for removing oxide from the silicon crystal surface and also possible residue of organic materials most of which presumably had been removed by the preceding heating in the vacuum.

After 15 minutes of plasma treatment, the hydrogen leak was closed. Liquid nitrogen was introduced into a Meissner trap in the system and the vacuum was reduced to 2×10^{-6} torr in about 15 minutes. m-Si deposition was then commenced.

In the present program, the main subject of study was highly doped p-type m-Si. The dopant used was boron which can be introduced in two ways. Initially intrinsic silicon (6) and boron from a graphite boat were co-evaporated (8). In the operation, an ac voltage of about 6 volts was applied acacross the graphite boat, leading to a current of about 120 amperes. The temperature near the hole where boron was placed was about 1800°C, depending on the desired electrical conductivity. The electrical power for the boron boat was determined empirically by correlation with the final surface electrical conductivity.

The second way to introduce boron was e-beam evaporation of heavily doped silicon. This method was developed because a large amount of carbon (in a range of high 10^{20} to 10^{21} atoms/cm^3) was measured at JPL in m-silicon films coevaporated with boron. The carbon concentration was determined by secondary ion microscopy. The same method was also used to determine boron concentration. There were several possible sources of this carbon. One was from the contamination of diffusion oil. This was unlikely because, firstly, the carbon concentration was excessively high, and secondly, the high carbon concentration occurred in the region of boron doping only. Alternatively, this carbon could have come from the graphite boat used for boron evaporation. According to vapor pressure data, at the temperature of 1800°C, the carbon vapor pressure was two orders of magnitude lower than that of boron. However, since the surface area of the high temperature region of graphite could have

been appreciable, carbon vaporization could have occurred while boron was evaporated. This estimate cannot explain the observed 10 to 100 ratios of carbon concentration to boron concentration. Nevertheless we decided to evaporate m-Si from a boron doped silicon source, to replace the two-source co-evaporation by a single source. The first trial with 0.1 ohm-cm silicon material gave a m-Si film of almost intrinsic conductivity, implying insufficient effective boron. Following this trial, pure boron, of about 0.1% was mixed with silicon in a graphite crucible and heated by electron beam to the melting temperature of silicon for about 10 minutes to produce a uniform boron-silicon alloy. This source produced a suitable p-type m-Si film. Since the electron beam is located at the center of the crucible away from the graphite crucible wall during evaporation, it is expected that graphite evaporation was minimized.

Runs 1 through 16 were made by coevaporation. From 17 to the end, the single source procedure to deposit p-Si was used. After two months of experiments, the quality of the solar cells produced by this new evaporation arrangement became as good as that by the coevaporation approach. Later testing at JPL showed that a large amount of carbon still existed. At this point, we still do not know whether the inclusion of carbon in m-Si is harmful or not.

In the later stage of the contract, preliminary tests on n-type m-Si deposition were made. Antimony was co-evaporated in a separated boat for doping. Since the melting temperature of Antimony was low, no contamination from the boat was expected.

Returning now to m-Si deposition. After the temperature monitored at the substrate holder, reached a predetermined value which was in the range of 580 to

620°C, the deposition was commenced with a deposition rate of about 500 Angstroms per minute. The total thickness or the deposition rate is monitored by a Sloan quartz thickness monitor located at the same distance from the source as that between the substrate and the source, but maintained at a distance from the cage to minimize the heat radiation from the cage-heater assembly.

After the deposition was completed, hydrogenation treatment of the samples was conducted either in situ or outside the vacuum system. In the case of in situ hydrogenation treatment the electrical power was lowered, and when the temperature had dropped to 400°C, a dc plasma of 3 kv, and 10 ma was introduced through the discharge rod (17). More recently, a discharge ring was introduced between shutter (10) and substrate holder (1), instead of the rod (17), for better plasma uniformity. The pressure in the system during the plasma treatment was maintained between 120 and 100 microns. The treatment time was one hour and after that period, the heater was disconnected and the temperature was reduced to 250°C in about five minutes; the plasma was then stopped and the in situ hydrogenation is completed. In the case of hydrogenation outside the vacuum system the electrical power of the vacuum system was disconnected after film deposition and when the temperature reached about 200°C, the samples were removed. The hydrogenation system was a pyrex tube capacitance coupled to a 13.6 MHz microwave power source. The pyrex tube was connected to a vacuum pump on the one end and a hydrogen source on the other end. The discharge power, the temperature and the pressure were about the same as the in situ dc plasma case. The results from the microwave treatment were generally better than the dc in-situ case at present.

IV. SOLAR CELL FABRICATION AND RESULTS

A. Cell Fabrication

During the course of this contract, various kinds of substrates were employed for various structures shown in Figure 1. All these substrates were prepared at ASEC. In the case of single crystal n-type or p-type substrates, they were polished and cleaned (only 1-3 ohm-cm n wafers were used but the p-wafer resistivity was varied). In the case of p-n junction or n-p junction substrates, appropriate diffusions were made. (For the p-n junction a 2 hour 920°C BN wafer diffusion with one hour annealing, and for the n-p junction a 10 min. 875°C $POCl_3$ diffusion was used). However, since there was an uncertainty about whether normal contact sintering temperature (400°C) could be applied to samples after m-Si deposition (for fear of dehydrogenation of the m-Si film), some samples were prepared to ensure good Ohmic back contacts on the end devices even with low temperature sintering. The first method tried was to deposit a metal contact on the back of the sample in the preparation stage using the high temperature process in the m-Si film deposition stage to provide contact sintering. This method was abandoned because of discoloring of the metal film after the heating cycle of the m-Si deposition. Another method tried was to make a high-low doping back junction in the preparation stage to ensure acceptable back contacts. For $n\text{-}n^+$ samples or $p\text{-}n\text{-}n^+$ samples, the n^+ layer was introduced by a short (6 min. 875°C) $POCL_3$ diffusion. For $n\text{-}p\text{-}p^+$ samples the p^+ layer was introduced by deposition of Al metal film and an 800°C, 15 minutes alloying. After preparation, the wafers were cut into 2" x 15/16" rectangles and were sent to Boston College for m-Si film deposition. After a number of runs, some of the samples were sent back to ASEC for cell fabrication. In each 15/16" x 2" sample only an area of about 4.8cm x 1.5cm was covered by the m-Si film. Therefore, usually only a number of small cells were fabricated on the covered

area. A total of six lots of samples were sent back to ASEC. In most cases, three to four 1x1cm cells were fabricated except in the 1st lot where 8 smaller cells were made, and part of the 6th lots where two 1x2cm^2 cells were made on the heteroface samples. For lots 1 to 5 only low temperature (220°C) contact sintering was used to reduce the chance of dehydrogenation (as mentioned above). However, heat treatment tests on selected solar cells indicated that no degradation of performance was observed after 2 hours heating at 350°C. Therefore, in the 6th lot, the contact sintering temperature was raised to 300°C. During the course of the contract, various sets of control cells were also fabricated for comparison. Some of their results will be presented with the m-Si cells results in the next section. No AR coating was used throughout the contract.

B. Solar Cell Results

Table 1* summarizes the condition of all the runs and also the resultant solar cell data. Table 2 gives the results of samples where small control cells were also fabricated on the area of the sample not covered by the m-Si films. Table 3 lists the results of a group of pnn$^+$ samples where the other halves from the same wafers were used as control for comparison. Table 4 is similar to Table 3 with npp$^+$ samples in complementary structures. The detail of these tables will be discussed in the following paragraphs.

1) Discussion On The Results Of The Heterojunction Structure

Table 1 gives an overview of all the results. The heterojunction structure (Figure 1a) with p m-Si on n or nn$^+$ substrates, was not very successful.

*All Tables are grouped at the end of the text.

The best Voc obtained was 482mV (in Run #4) with more than half of the samples showing low Voc (200mV and below) throughout the contract. From the original data the low Voc samples were mostly caused by severe shunting while most of the IV curves for the higher Voc (>200mV) samples had large curvature and indicated a poor junction interface. Examining Table 1, the higher Voc samples in general had thicker m-Si films (the thickness of the films was measured by the shift of quartz crystal resonance frequency in kc units with about 0.3 microns for each change/kc). This suggested that shunting paths such as pinholes in the film might be the source of the shunting for the thinner m-Si films while in the thicker films, this problem was reduced. As for the interface problem, it will be discussed in more detail later. Preliminary tests on the complementary structure with n-type m-Si film on p-type samples only produced Voc values up to 230mV (n-type m-Si film is indicated by "n" under the Run # in Table 1).

2. Discussion On Results Of The Heteroface Structure

For the heteroface structure (Figure 1b, p-type m-Si film on p-n or p-n-n+ substrate), the best Voc achieved was about 570mV which was below the best control cells (in the 590mV range). Nevertheless, careful comparison of controls cut from the same wafers of the heteroface cells presented a different picture. Table 2 presents the result of the first test. Since the m-Si film does not cover the whole sample, small solar cells can be fabricated from the area not covered by the m-Si film. Two samples were selected. Three m-Si solar cells were fabricated in each sample and each m-Si solar cells has two adjacent smaller cells not covered by m-Si. From Table 2, for sample J-39, the m-Si cells were better than the adjacent

cells while for sample J43 they are similar in Voc, but lower in Jsc than the adjacent cells. There were certain questions about the results of this test because of the low performance of the adjacent cells compared with other controls. This adjacent area was in contact with the metal frame during the m-Si film deposition and contamination was possible. Therefore, another test was conducted. Since each 3" wafer could be cut into two standard samples, after the appropriate diffusions, one was sent for m-Si deposition and one was saved as a control. After m-Si deposition, both sets of samples were processed together. The results are summarized in Table 3. For samples T2, T3 and T4, three $1x1cm^2$ cells were fabricated on the m-Si film of each sample and up to six cells were fabricated on the control sample because there is no geometric limitation. For the rest of the samples, two $1x2cm^2$ cells were fabricated on m-Si sample and up to four similar cells on the control. (The $1x2cm^2$ cell has a substantially larger percentage of active area, but this proves not to be a major factor.) From Table 3, three samples (T2, T5, T10) showed sign of improvement in Voc on the m-Si samples with sample T3 being the strongest. In all cases, Jsc was lower for the m-Si cells due to the extra absorption of the m-Si film, combined with less effective collection by transport through the m-Si layer. This lower Jsc limited the efficiency of the m-Si cell even with higher Voc. The enhancement of Voc would have been slightly higher if the Jsc values were comparable. Besides the three samples listed above, all the rest of the samples had lower Voc. Therefore, even though there was some promise, it was still very inconsistent and any voltage increase was too small to compensate for the loss of current due to the film. Nevertheless some voltage enhancement seemed to occur due to the m-Si film.

For the complementary structure (n-type m-Si film on n-pp$^+$ substrate), similar tests with m-Si and control samples cut from the same wafer were conducted. The results are listed in Table 4. The cell size was 1x2cm^2. To date no voltage enhancement was observed in this preliminary test.

3. Discussion Of The Results Of The p m-Si/p-Substrate (or n m-Si/n substrate) Test Structures

The motivation for studying this testing structure (Figure 1C) was to isolate out the p m-Si/p interface from the heteroface structure and to see how this p/p heterojunction functions. This structure also reduced any PN junction effects and was thus a pure heterojunction. The results of this structure can be found from Table 1, in lot 4 and 5, with p-type m-Si runs ("P" appear under the Run #) and P substrates. A wide range of resistivities of P samples was used in this test including 0.15, 1-3, 7-14 ohm-cm. The average resistivity of the group where that sample belongs is listed under the substrate type after "P" e.g., p10 means P substrate with 10 ohm-cm (7-14 ohm-cm). There were some curious results for this structure. A few substrates produced cells with only a few mV of positive voltage. All the rest had negative measured Voc values i.e. opposite to that expected for a wide gap P-semiconductor on a lower gap P-semiconductor. This negative or "wrong" polarity is indicated by parentheses and fairly large negative Voc up to 100mV were recorded. This might imply that instead of repelling minority carriers from the p substrate, the junctions actually collected some of them and produced a negative Voc (the front contact was found to be ohmic in a separate study and could not be the source of this phenomenon). In a heterojunction, such effects are possible depending on the conditions at the interface.

Therefore the effectiveness of the m-Si layer as a minority carrier barrier is probably dominated by this phenomenon. This could be the source of the inconsistency of the results in the heteroface cells. In a few isolated cases, this negative polarity in Voc was also observed in heterojunction cells (p-type, m-Si/n). However, in those runs (Run #19 and 20), the boron doping might not be high enough.

In the complementary structure (n-type m-Si p on n substrate), this opposite (in this case positive) polarity phenomon was also observed in Runs 33 and 35 and presumably can also be a minority carrier collection from the substrate. These tests show that there are still many questions about the properties of the interface between m-Si and c-Si to be answered.

6. Back-Up Measurements

Various back-up measurements were made during the contract. Preliminary tests on the sheet resistance of p-type m-Si film on some samples by a transmission line model gave values of 880-1000 ohm/□. Also a number of solar cells was subjected to a 2 hour, 350°C heat treatment test as mentioned earlier. There was no indication of deterioration in performance of these cells. Therefore, our earlier fear of m-Si dehydrogenation at higher temperatures was probably invalid. On the other hand, preliminary photovoltage measurements (just point contacts without metal electrodes) at Boston College indicated that hydrogenation was still important, because there was consistent improvement after hydrogenation even though the measurement was only comparative. A test on the effect of the film deposition heat cycle was conducted by placing covered substrates in the chamber in Runs 29 and 30, the resultant Voc was not

different from the controls made in similar wafers as shown in Table 2. Therefore the heating effects were minimal.

Another back-up measurement was spectral response measurement on selected samples. Figures 4, A and B, both show the spectral responses of a heteroface cell and a control cell cut from the same wafer. In both cases, on the short wavelength side, the cell with m-Si film had substantially lower response due to the film absorption and incomplete collection, even though on the long wavelengths side, one cell had higher and one cell had lower response than their respective controls. We will not attempt to correlate the cross over point in these responses with the supposed bandgap of the m-Si film. The cross over point in Figure 4A is 0.78um equivalent to 1.59eV which is lower than 1.7eV. For Figure 4B, the exact position of the cross over point is not sure.

The last back-up measurement to be mentioned here is a dark current measurement as shown in Figures 5A and B. Figure 5A shows the dark currents of the heterojunction cells with high A (diode quality factor) values and some series resistance. High A-values point to interface problems in the junction. Figure 5B shows heteroface cells, and their characteristics are similar to the control solar cells as expected. The particular cells chosen here are from samples where Voc enchancement was observed and this is also seen in Figure 5B.

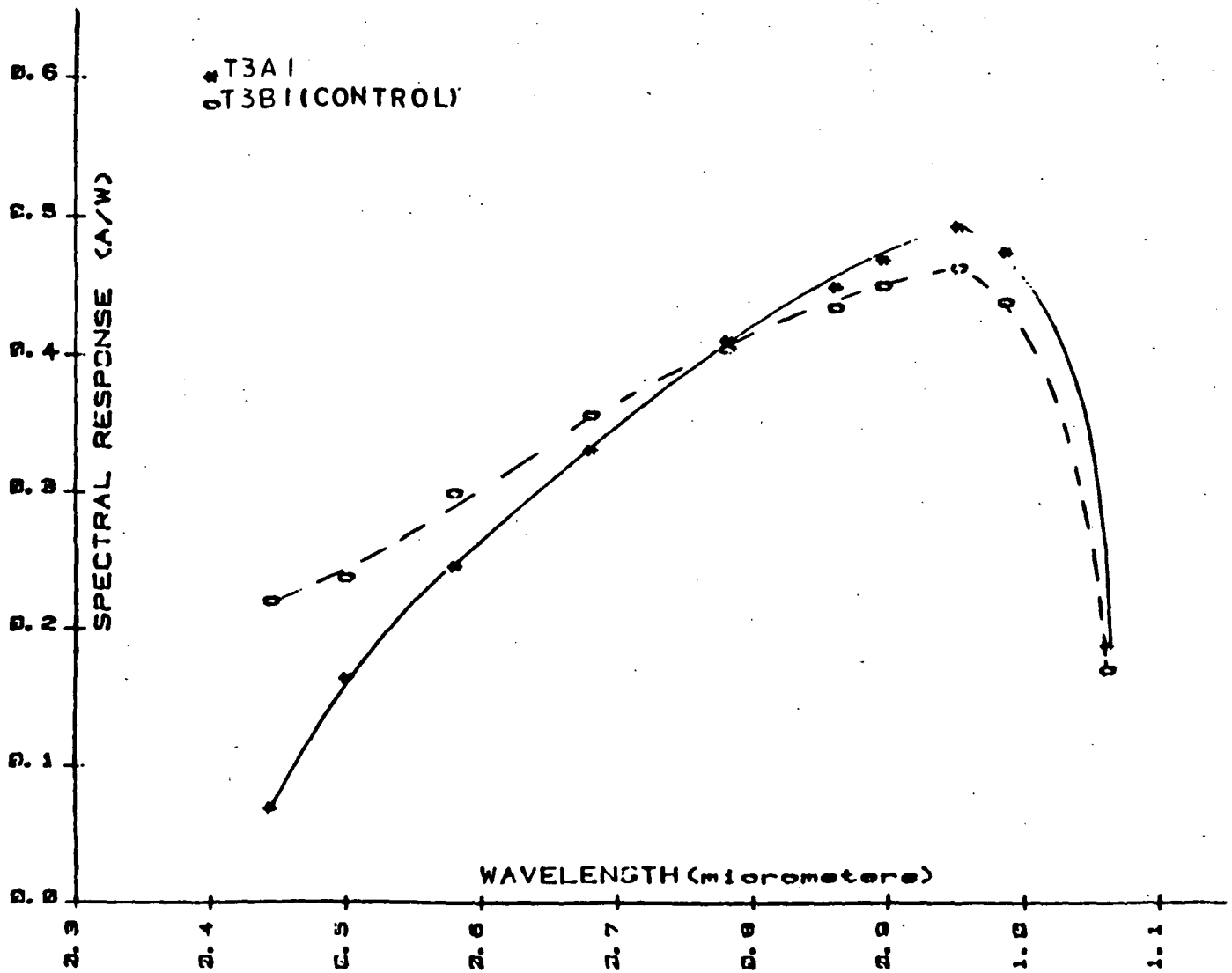

FIGURE 4A

SPECTRAL RESPONSES OF SELECTED HETEROFACE CELLS

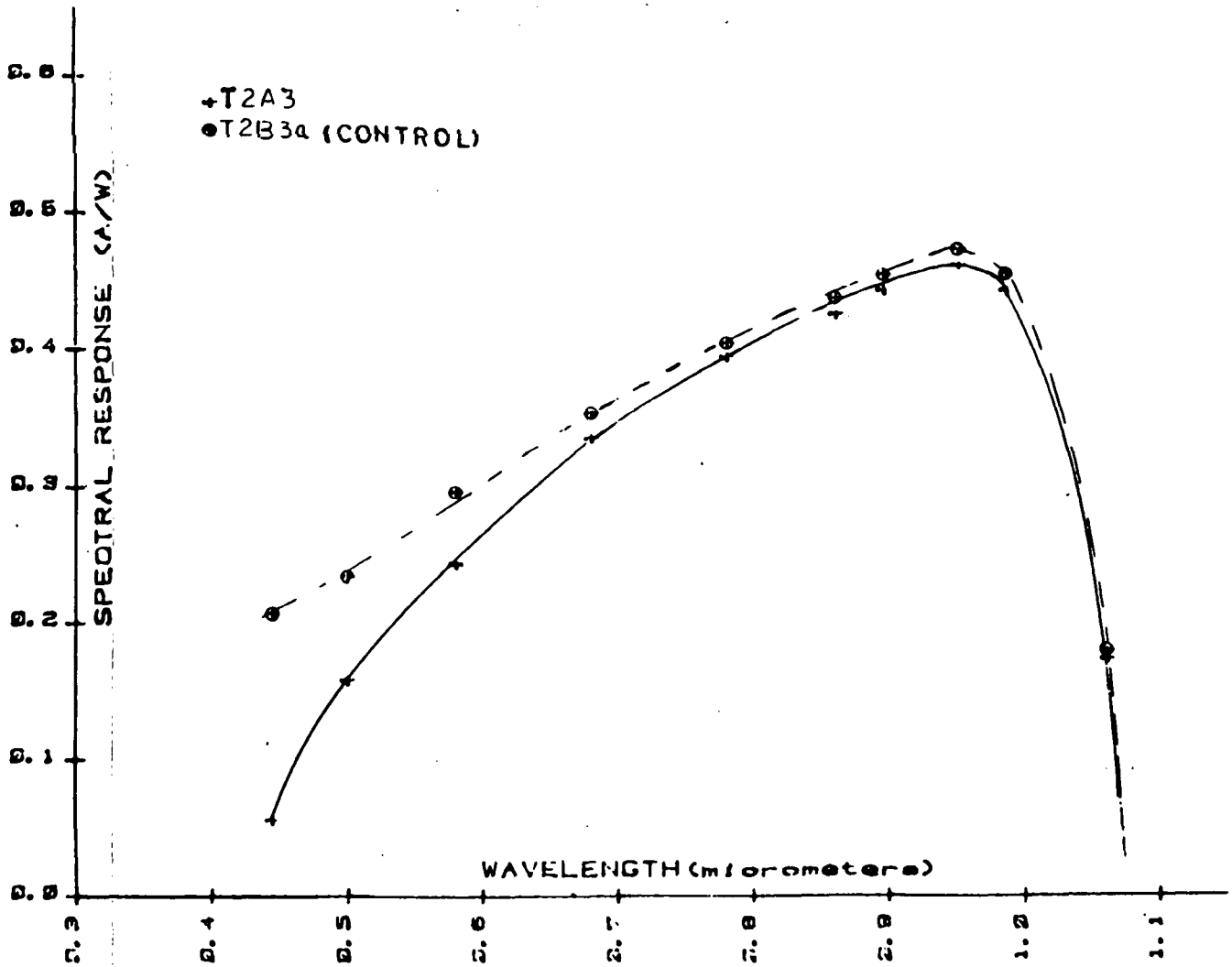

FIGURE 4B

SPECTRAL RESPONSE OF SELECTED HETEROFACE CELLS

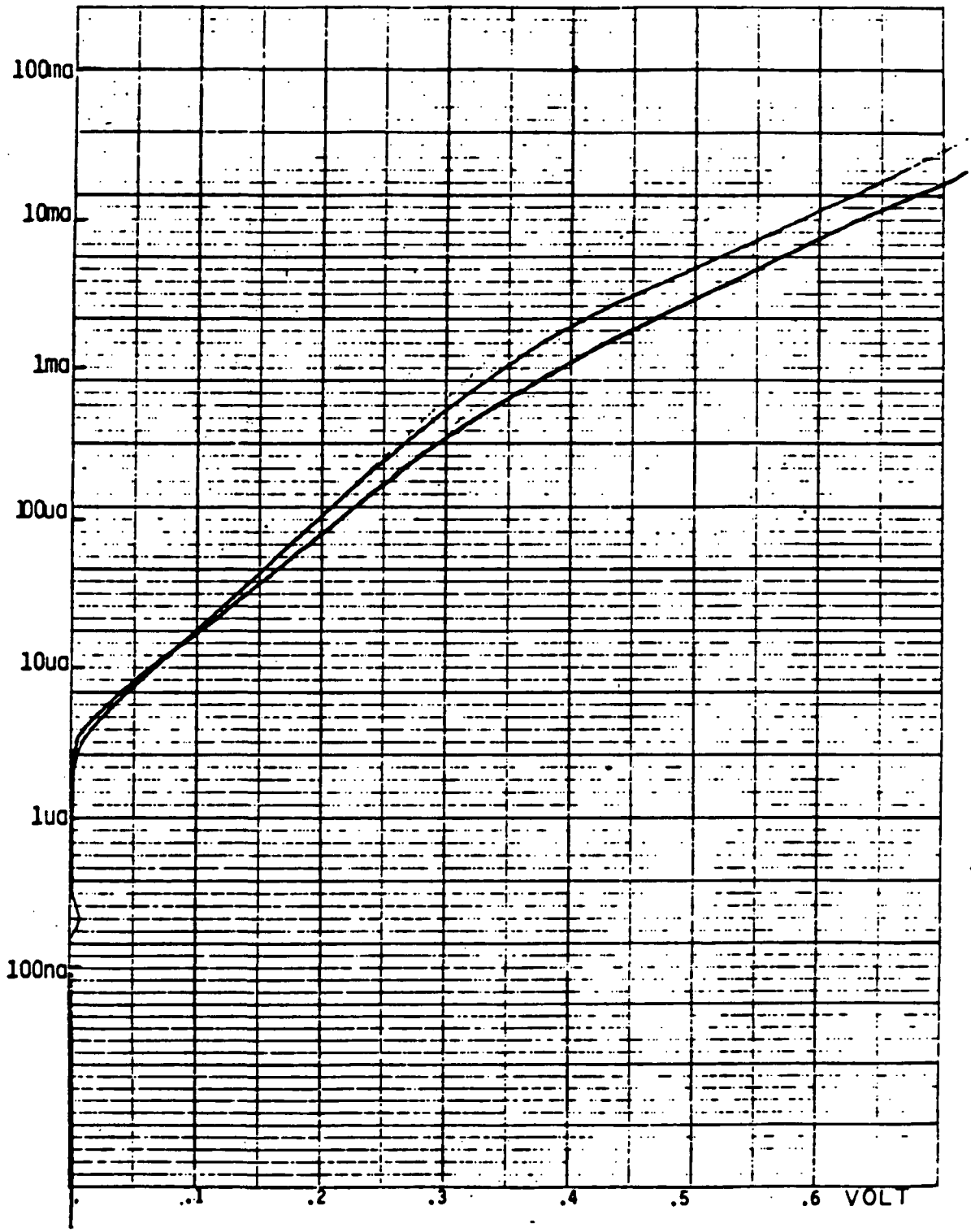

FIGURE 5A

DARK CURRENTS OF SELECTED HETEROJUNCTION CELLS

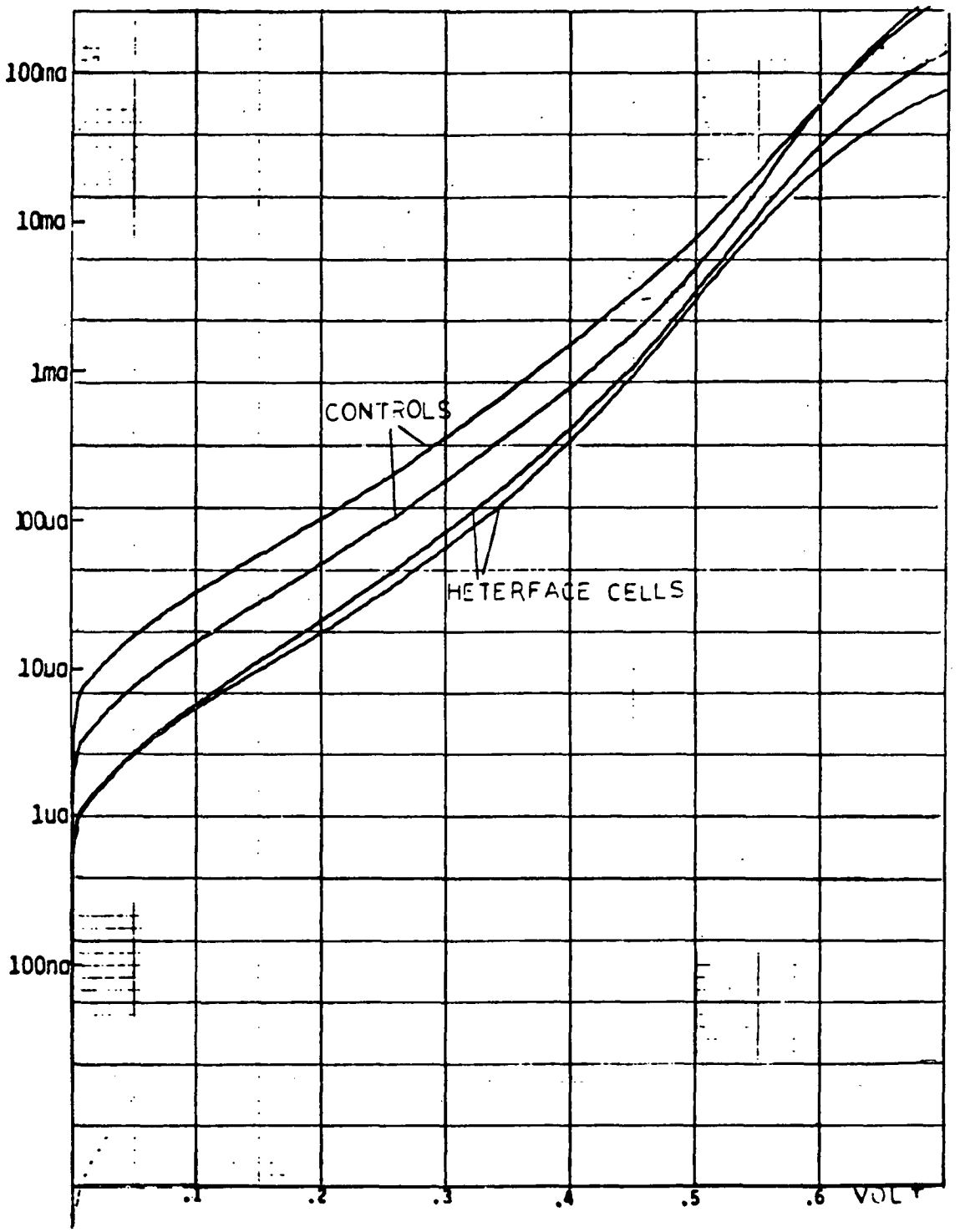

FIGURE 5B
DARK CURRENTS OF SELECTED HETEROFACE CELLS
AND CONTROL CELLS

V. CONCLUSIONS

This contract set out to test m-Si film as a Voc enhancer either in a heterojunction to crystalline Si or as a window layer in a heteroface structure. The heterojunction structure could produced Voc values only up to about 480mV, and was troubled by shunting and poor junction quality. For the heteroface structure, there was some promise shown in direct comparison, but the results were inconsistent and in general, the Voc enhancement observed was not enough to compensate for the loss of current due to extra absorption and poorer transport in the m-Si film. Some preliminary study on the complementary structures showed no positive results. The results of the p-type m-Si on P substrate test structures and its complement showed that there were a lot of unanswered questions concerning the interface between the m-Si c-Si interface, as illustrated by the existence of Voc of the opposite polarity in many of the samples. Until some of these questions are answered, it cannot be decided whether there is any prospect for improvement.

This contract has shown that more information must be acquired before these approaches to improve solar cell performance can be implemented.

VI. REFERENCES

1. P.H. Fang, L. Ephrath and W.B. Nowak, Appl. Phys. Lett. 25, 583 (1974).
2. J.I. Pankove, Appl. Phys. Lett. 32, 439 (1978).
3. P.H. Fang, C.C. Schubert, J.H. Kinnier and Dawen Pang, Appl. Phys. Lett. 39. 256 (1981).
4) Y. Nagarta, A. Kunioka and S. Yamazaki, Appl. Physa. Lett. 38, 142 (1981).
5) Y. Uchida, T. Ichimura, M. Ueno and M. Ohsawa, Proc. 9th Intern. Conf. Amorphous and Liquid Semiconductors (Grenoble, France 1981, B.K. Chakraverty and D. Kaplan, Eds.) p. C4-265.
6) R.A. Forman, W.R. Thurber and D.E. Aspness, Solid State Comm. 14, 1007 (1974).
7) Z. Iqbal, A.P. Webb and S. Veprek, Appl. Phys. Lett. 36, 163 (1980).
8) R. Richter and L. Ley, J. Appl. Phys. 52, 7281 (1981).
9) P.H. Fang, C.C. Schubert, Peiguang Bai and J.H. Kinnier, Appl. Phys. Lett. 41, 356 (1982).
10) A. Matsuda, K. Kumagai and K. Tanaka, Jpn. J.A.P. Letters 22, 34 (1983).
11) P.H. Fang, Peiguang Bai, C.C. Schubert and J.H. Kinnier, Jpn. J. Appl. Phys. (To appear.).
12) T. Hamasaki, H. Kurata, M. Hirose and Y. Osaka, Appl. PHys. Lett. 37, 1984 (1980).
13) J. Gonzalex-Hernandez and Raphael Tsu, Appl. Phys. Lett. 42, 90 (1983).
14) H. Richter and L. Ley, J. Physique, Coll. C1, Suppl. 10, 43, 247 (1982).

TABLE 1

SUMMARY OF RUN CONDITIONS AND CELL RESULTS (UNCOATED CELLS)

Run	Position	ASEC #	Type	M-Si Deposition		ASEC Cells		
				Temperature (°C)	Thickness (kc)*	Voc(mV) Range	Jsc(mA) Range	Lot No.
1				616	1.10			
	A	2	n					
P-Type	B							
Film	C	31	n					
	D	32	n			13	1.3-11.3	1
	E	1	n					
2				647	1.35			
	A	3	n			26	1.4-18.6	1
P-Type	B							
	C	33	n			30	4.4-15.1	1
Film	D	34	n			4	3.9-7.5	1
	E	4	n			38-107	9.5-19.0	1
3				635	2.40			
	A							
P-Type	B							
	C							
Film	D							
	E							
4				647	2.70			
	A	37	n			210-298	13.9-14.1	
P-Type	B	38	n			198-344	12.9-13.1	2
	C	39	n			254-460	9.8-13.3	2
Film	D	40	n			414-482	12.6-12.9	2
	E	42	n					
5				642	2.80			
	A	7	n			20-202	8.6-13.3	2
P-Type	B	8	n			340-426	14.3	2
	C	9	n			20-60	8.8-14.1	2
Film	D	10	n			402-428	148-15.1	3
	E	11	n			322-356	11.7-14.7	3
6				635	2.30			
	A	43	n			376-410	14.5-14.7	3
P-Type	B	44	n			40-111	2.4-8.4	2
	C	45	n			20-414	0.8-14.3	2
Film	D	46	n			20-116	0.9-8.2	2
	E	47	n					

*1kc corresponds to about 0.3 microns in thickness.

Run	Position	ASEC #	Type	M-Si Deposition		ASEC Cells		
				Temperature (°C)	Thickness (kc)*	Voc(mV) Range	Jsc(mA) Range	Lot No.
7				636	0.60			
	A							
P-Type	B							
	C							
Film	D	13	n			114-216	10.4-14.1	2
	E	46	n					
8				602	0.50			
	A							
P-Type	B							
	C							
Film	D	48	n					
	E	14	n			60-84	17.2-17.7	2
9								
	A	M3	n*	630	1.70			
P-Type	B							
	C	JPL	n			260-275	2	3
Film	D	M4	n*					
	E	JPL	n					
10				644	1.90			
	A	n	q			48-308	1	3
P-Type	B							
	C	JPL	n					
Films	D	M8	n*			20-80	0.05-2.4	*
	E	M7	n*			80-92	0.8-12	*
11				652	1.80			
	A	15	n			201-216	1.7	3
P-Type	B							
	C	50	n			20-161	1	3
Film	D	JPL						
	E	16	n			140-182	1.8-7.9	3
12				626	2.40			
	A	49	n			121-134	1	3
P-Type	B							
	C	17	n			91-149	1.1	3
Film	D	18	n			77-91	1.3	3
	E	M6	n*					
13				640	1.00			
	A	51	n			123-180	1	3
P-Type	B							
	C	19	n			197-225	1	3
Film	D	JPL				73-166	1	3
	E	M5	n*			73-166	1	*

*These samples had metal back contact before m-Si film deposition.

Run	Position	ASEC #	Type	M-Si Deposition		ASEC Cells		
				Temperature (°C)	Thickness (kc)*	Voc(mV) Range	Jsc(mA) Range	Lot No.
14				652	.54			
	A	J15	pn			530-550	13.7-17.0	3
P-Type	B							
	C	52	n			158-254	2.2	3
Film	D	J12	pn			546-538	14.5-16.9	3
	E	J28	pn			526	13.5	*
15				652	.60			
	A	J14	pn			506-532	13.9-16.3	3
P-Type	B							
	C	53	n			134-296	1	3
Film	D	J13	pn			428-476	10.013.2	3
	E	J27	pn*			538-544	13.1-13.3	*
16				649	.43			
	A	J10	pn			528-546	16.4-16.5	3
P-Type	B							
	C	54	n			204-232	2.0	3
Film	D	J11	pn			508-528	14.1-16.9	3
	E	J27	pn*			338-544	13.1-13.3	*
17				626	2.40			
	A	40	pnn+					
P-Type	B							
	C	20n				96-328	14.5-18.2	4
Film	D	70	nn+			216-316	16.6-18.2	4
	E	38	pnn+					
18				616	0.39			
	A	69	nn+			20	0.1	4
P-Type	B		p.01**					
	C	21	n			100-120	1.6-4.7	
Film	D	J39	pn			570	19.2-19.3	4
	E	55	np					
19				621	0.49			
	A	56	nn+			1-3	0	4
P-Type	B							
	C	22	n			(3) to +2	0	4
Film	D	J37	pn			342-404	16.8-17.0	4
	E	56	n			(75)-(12)*	(0.1)+(.7)	4
20				628	0.70			
	A	68	nn+					
P-Type	B		p.01					
	C	23	n			(52) to 2	0 to.03	4
Film	D	J36	pn			258-328	16.5-17.0	4
	E	57	n			(1) to 0	(0.3)to 0.1	4

** For the P samples, the numbers that follow the letter "P" are the approximate resistivity.

+All Voc and Jsc values in the parenthesis are values of the opposite polarity to what were supposed to be.

Run	Position	ASEC #	Type	M-Si Deposition		ASEC Cells		
				Temperature (°C)	Thickness (kc)*	Voc(mV) Range	Jsc(mA) Range	Lot No.
21				607	.70			
	A	24	n			0	0	4
P-Type	B	J41	pn			156-168	17.6	4
	C	P1	p.15					
Film	D	p21	p10					
	E	p11	p2					
22				593	2.24			
	A	P2	p.15					
P-Type	B	25	n			250-326	13.0-14.7	4
	C	66	nn+			338-460	14.1-14.9	4
Film	D	J42	pn			564-572	14.8-15.6	4
23*				612	1.72			
	A	P28	P10					
P-Type	B	P7	P.15					
	C	P17	P2			(146)-(120)	(9.3)-(8.0)	4
Film	D	J45	pn			548-564	15.7-15.9	4
	E	65	nn+					
24				623	2.35			
	A	P27	P10			(110)-(80)	(8.6)-(4.1)	4
P-Type	B	P4	P.15					
	C	P16	P2					
Film	D	J47						
	E	64	nn+					
25				614	2.08			
	A	P3	P.15			(116)-(94)	(8.6)-(6.7)	4
P-Type	B	26	n			132-148	14.3-15.1	4
	C	59	n			98-112	11.8-13.9	4
Film	D	J43				552-558	15.1-15.3	4
	E	63	nn+					
26				612	2.0			
P-Type	A	P8	P.15					
	B	27	n					
Film	C	60	n					
	D	J44	pn			554-558	14.1-14.3	4
	E	61	nn+					
27				588	0.38			
	A	100	nn+					
n-Type	B	99	nn+					
	C	P5	P.15					
Film	D	P25	P10			20-60	0.1	5
	E	J48	n+np					

*In run 23 on, the boron content in p-Si source crucible has been increased for P-type film.

Run	Position	ASEC #	Type	M-Si Deposition		ASEC Cells		
				Temperature (°C)	Thickness (kc)*	Voc(mV) Range	Jsc(mA) Range	Lot No.
28				576	0.33			
	A	98	nn+			14-25	0.1-0.8	5
n-Type	B	28	n			7-28	0.3-1	5
	C	P6	P.15					
Film	D	P26	P10					
	E	97	n+n					
29		Covered		576	0.30			
	A	T5A	pnn+			558-562	21.3-21.7	5
n-Type	B	T4A	pnn+			554-562	19.2	5
	C	T3A	pnn+			566-570	19.0-19.6	5
Film	D	95	nn+			82-180	18.2-18.6	5
	E	96	nn+					
30		Covered		572	0.24			
	A	T1A	pnn+			562-564	21.5-21.9	5
P-Type	B	T2A	pnn+			556-568	19.1-19.4	5
	C	92	nn+			196-370	18.4-19.4	5
Film	D	93	n+n			1	4-6	5
	E	29	n					
31				595	0.24			
	A	P23	P10			60-226	0-0.6	5
n-Type	B	P24	P10					
	C	P18	P2					
Film	D	30	n					
	E	P12	P2			208-230	3.0-5.5	5
32				623	0.30			
	A	112	nn+			0.2	0.1-1.7	6
P-Type	B	T10A	pnn+			558-564	20.5-20.8	6
	C	T9A	pnn+			494-498	22.0-22.3	6
Film	D	T8A	pnn+			554	20.0-20.2	6
	E	111	nn+			210-312	20.2-20.8	6
33				633	0.30			
	A	110	nn+			(30)-(42)	(10.0)-(13.9)	6
n-Type	B	N1A	npp+			566-568	19.2-19.4	6
	C	107	nn+			0	(1.2)-(2.6)	6
Film	D	N5A	npp+			552-560	18.5-19.0	6
	E	N4A	npp+			568-570	18.0-18.2	6
34								
	A	T13A	pnn+					
P-Type	B	107	nn+			32-50	6.4-19.0	6
	C	108	nn+			22-318	16.3-20.9	6
Film	D	T6A	pnn+					
	E	T7A	pnn+			558-560	21.4-21.6	6
35								
	A	87	nn+			0-(30)	(0.6)-(1)	6
n-Type	B	88	nn+			(66)-(108)	0-(15.5)	6
	C	N3A	npp+			20-568	9.2-18.9	6
Film	D	N2A	npp+			570	18.9-19.4	6
	E	86	nn+			(74)-(84)	(8.5)-(9.6)	6

TABLE 2

COMPARISON OF SOLAR CELLS COVERED BY m-Si WITH ADJACENT SOLAR CELLS MADE IN AREA NOT COVERED BY m-Si

		Voc (mV)	Jsc (mA/cm^2)	CFF (%)	n (%)
J-39-1 (m-Si Covered)		570	19.2	76	8.3
Adjacent Cells (Not Covered by m-Si)	a	552	20.2	63	7.0
	b	548	16.3	71	6.4
J39-2 (m-Si)		570	19.2	75	8.2
Adjacent Cells	c	550	19.2	65	6.9
	d	544	17.8	69	6.6
J39-3 (m-Si)		570	19.3	73	8.1
Adjacent Cells	e	548	17.9	71	7.1
	f	558	19.2	71	7.5
J43-1 (m-Si)		558	15.4	77	6.7
Adjacent Cells	a	552	17.5	71	6.7
	b	558	16.8	75	6.7
J43-2 (m-Si)		552	15.1	74	6.2
Adjacent Cells	c	554	18.0	74	7.5
	d	556	19.4	71	7.7
J43-3 (m-Si)		552	15.3	73	6.1
Adjacent Cells	e	552	19.1	71	7.5
	f	562	19.6	75	8.3

TABLE 3

COMPARISON OF HETEROFACE (p m-Si/p-n-n+) CELLS

WITH CONTROLS MADE FROM THE SAME WAFERS

WAFER		Cells With m-Si Window Layer		Control Cells	
		Voc (mV)	Jsc(mA/cm^2)	Voc (mV)	Jsc (mA/cm^2)
T2	Ave.	563	19.2	561	21.5
	Range	556-568	19.1-19.4	560-562	21.1-21.7
T3	Ave.	569	19.3	555	20.9
	Range	566-570	19.0-19.6	550-558	20.4-21.3
T4	Ave.	559	19.2	562	21.5
	Range	554-562	19.2	560-564	21.3-21.5
T7	Ave.	559	21.5	562	22.4
	Range	558-560	21.4-21.6	562	22.3-22.5
T8	Ave.	554	20.1	563	22.6
	Range	554	20.0-20.2	562-564	22.6-22.7
T9	Ave.	596	22.2	562	22.4
	Range	494-498	22.0-22.3	560-562	22.2-22.5
T10	Ave.	561	20.7	560	22.3
	Range	558-564	20.5-20.8	556-562	22.2-22.4

TABLE 4

COMPARISON OF COMPLIMENTARY HETEROFACE (n m-Si/n-p-p+) CELLS

WITH CONTROLS MADE FROM THE SAME WAFERS

WAFER		Cells With m-Si		Control Cells	
		Voc (mV)	Jsc(mA/cm^2)	Voc (mV)	Jsc (mA/cm^2)
N1	Ave.	567	19.3	574	22.4
	Range	566-568	19.2-19.4	574	22.3-22.4
N2	Ave.	570	19.2	577	22.6
	Range	570	18.9-19.4	576-578	22.5-22.8
N3	Ave.	568	18.9	574	22.5
	Range	-	-	572-576	22.3-22.8
N4	Ave.	569	18.1	580	22.8
	Range	568-570	18.9-18.2	-	-
N5	Ave.	556	18.8	572	22.6
	Range	552-560	18.5-19.0	570-572	22.4-22.9